Proceedings of the 2003 IEEE International Frequency Control Symposium and PDA Exhibition
Jointly with the 17th European Frequency and Time Forum

NEW FREQUENCY COMPARISONS USING GPS CARRIER-PHASE TIME TRANSFER

Christine Hackman[1] and Judah Levine[2]
[1]JILA, University of Colorado, Boulder, Colorado, USA
[2] JILA and National Institute of Standards and Technology, Boulder, Colorado, USA

Abstract - **In October 2002, experiments were conducted to assess the frequency accuracy available from GPS carrier-phase time transfer (GPSCPTT). In these experiments, two GPS receivers, NIST_A and NIST_B, were operated in close proximity with one clock, UTC(NIST), serving as the receiver clock for both. Because the same clock was used for both receivers, the resultant time series Clk(NIST_A) – Clk(NIST_B) is expected to have a slope (frequency difference) of zero.**

The experiment yielded mixed results. Data recorded 22-25 October 2002 yielded slopes in the 12-24 ps/d range with both positive and negative signs, indicating that if one averaged long enough, the frequency error obtained from GPSCPTT might average out to zero. However, data recorded 5-9 October 2002 yielded slopes in the 45-77 ps/d range, with all of the slopes having the same sign. Thus, it appears that some sort of systematic frequency error is arising in either the measurement or data-analysis process.

Attempts have been made to determine the cause of this systematic error. Potential sources investigated include (a) unequal sampling rates at the two receivers, (b) the analysis technique of fixing satellite-clock corrections to predetermined values rather than estimating them, and (c) errors in the estimation of the tropospheric delay. None of these appear be the root cause of the problem. Future work will include the investigation of site- and receiver-specific effects such as temperature sensitivity and multipath.

Keywords **- GPS carrier phase time transfer, GPSCPTT, frequency, accuracy**

I. INTRODUCTION

One of the central goals of the NIST GPS carrier-phase time-transfer program is to compare primary frequency standards located at different timing laboratories. These standards realize the SI second with a fractional frequency uncertainty of about 10^{-15}, i.e., 86 ps/d. Therefore, one would hope that the measurement technique would be accurate in the frequency sense to at least one-half of that: 43 ps/d. One-tenth, 8.6 ps/d, would be preferable.

In October 2002, we performed experiments to determine whether the accuracy available from this technique was comparable to the accuracy required for the comparison of primary frequency standards. During this period, we operated two Ashtech Z-12T[1] timing receivers using UTC(NIST) as the clock for each receiver. Because a common clock was used, the measurement should yield a frequency difference of zero.

In this paper, we first describe the data collection and analysis. We then present the results and discuss possible sources of error.

II. EXPERIMENTAL SETUP AND DATA COLLECTION

From 1-26 October 2002, two Ashtech Z-12T timing receivers were operated at NIST in Boulder, Colorado. While the two receivers had separate antennae, a single "clock," UTC(NIST), was used to run both. Fig. 1 shows the details, which are as follows:

1 PPS and 5 MHz signals from UTC(NIST) were sent to receivers "NIST_A" and "NIST_B." Because the Ashtech

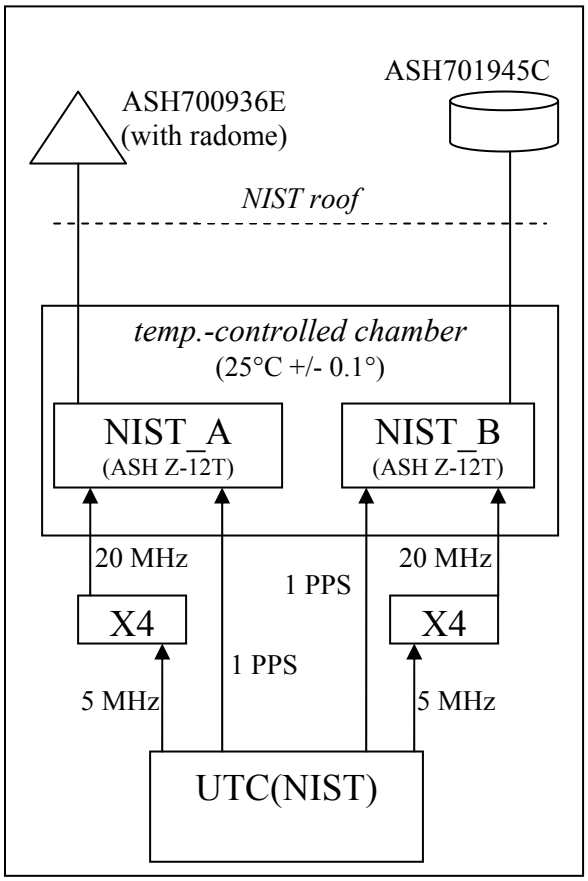

Fig. 1. Setup of the common-clock experiment. A single clock, UTC(NIST), was used as the receiver clock for two Ashtech Z-12T GPS receivers, NIST_A and NIST_B. The receivers were placed in a temperature-controlled chamber; while the receivers and clock were indoors, the antennae were outdoors on the NIST roof. The receivers had different antenna types as marked.

[1] The use of a specific trade name is for identification purposes only; no endorsement is implied.

Z-12T requires a 20 MHz input, the 5 MHz signals were multiplied prior to entering the receivers.

The delay through an Ashtech Z-12T receiver can vary with temperature [1]. Therefore, the NIST_A and NIST_B receivers were operated within the same temperature-controlled chamber. The temperature of the chamber was maintained at 25°C with a stability of +/- 0.1°C.

While the two receivers were placed indoors, their respective antennae were placed outdoors on the NIST roof. The NIST_A receiver utilized an Ashtech 700936 Rev. E choke-ring antenna with a snow radome, whereas the NIST_B receiver utilized an Ashtech 701945 Rev. C choke-ring antenna with no radome. (See Table 1 for a summary of this and other differences between the two receiver-antenna pairs.)

The two antennae were spaced about 18 m apart in the horizontal direction and about 5.5 m apart in the vertical. NIST_B was the higher of the two and was located southwest of NIST_A. While the NIST_B antenna tracked all satellites above the horizon, the NIST_A antenna tracked only satellites with an elevation angle of 20° and higher. Both receivers recorded C/A-code, P1, P2, L1 and L2 data.

We present results from two different periods: 5-9 October and 19-25 October 2002. During the former period, the NIST_A receiver recorded GPS data every two seconds and the NIST_B receiver recorded data every 30 seconds. During the latter period, both receivers recorded data every 30 seconds. At each receiver, the data were recorded in one-day files, with a new file starting each day at midnight GPS time.

The data were recorded in the native Ashtech binary format and then converted to the standard ASCII RINEX format [2] using *TEQC* [3]. Thus, for each day, we obtained two RINEX data files: one for the NIST_A receiver and one for the NIST_B receiver. After these two data files had been processed, what we obtained for that day was a time series of Clk(NIST_A) – Clk(NIST_B)—a time series expected to have a slope of zero.

III. Data Analysis

The data were analyzed in 24-hour batches using *GIPSY* software developed at the Jet Propulsion Laboratory (JPL) [4]. We obtained satellite orbits, satellite-clock corrections and earth-orientation parameters from JPL; antenna phase center corrections were obtained from the National Geodetic Survey.

TABLE I
DIFFERENCES BETWEEN RECEIVERS NIST_A AND NIST_B

	NIST_A	NIST_B
Antenna type	Ashtech 700936E + snow radome	Ashtech 701945C
Elevation mask[A]	20°	0°
Sampling rate[B]:		
5-9 Oct 02	two seconds	30 seconds
19-25 Oct 02	30 seconds	30 seconds

[A]The elevation angle (relative to the horizon) above which the receiver tracked satellites.
[B]The time interval between subsequent GPS measurements.

To begin the analysis, the data files from the NIST_A and NIST_B receivers were edited for cycle slips. The pseudorange data (P1, P2) were then carrier-smoothed from the original sampling rate of one data point every two (or 30) seconds to a final rate of one point every five minutes; the carrier-phase data (L1, L2) were decimated from the original sampling rate to the final rate. The delay due to the ionosphere was then removed from the carrier-phase data by forming the "ionosphere-free" linear combination of the L1 and L2 data [5]; the ionospheric delay was removed from the pseudorange data by forming the corresponding linear combination of the P1 and P2 measurements [6].

With the data now properly prepared, the least-squares estimation was carried out. We estimated three sets of parameters: antenna coordinates, zenith tropospheric delays, and the time difference ("offset") between each of the receiver clocks and a reference clock. It is this last set of parameters that ultimately yields the quantity of interest, Clk(NIST_A) – Clk(NIST_B). The integer-cycle carrier-phase ambiguities were resolved as part of the analysis [7].

Antenna coordinates were estimated as constants. In other words, for each 24-hour batch of data, we obtained one set of x, y and z coordinates for the NIST_A antenna and another set for the NIST_B antenna.

The zenith tropospheric delay can be expressed as the sum of two parts: a "wet" part caused by the dipole component of water vapor refractivity and a "hydrostatic" part caused by dry gases and the non-dipole component of water vapor refractivity [8]. The wet part varies rapidly, whereas the hydrostatic part varies slowly.

The wet part of the zenith tropospheric delay was estimated at each of the two sites as a time-varying random-walk parameter. New values were estimated every five minutes; therefore, the analysis of a 24-hour batch of data yielded two 288-point time series: one representing the wet zenith tropospheric delay at the NIST_A antenna and another representing the corresponding delay at the NIST_B antenna.

Because the hydrostatic part of the zenith tropospheric delay varies slowly in time, it was not estimated. Rather, each site was assigned a fixed value based on height. Therefore, if the hydrostatic part of the tropospheric delay changed during the day, that variation was expressed as a variation in the estimated value of the wet zenith tropospheric delay.

The delay through the troposphere was assumed to be azimuthally symmetric; the Niell mapping function was used to model the elevation-angle dependence [9].

We now address the estimation of the receiver-clock offsets. Although this problem is treated as if the clocks running the NIST_A and NIST_B receivers were separate entities, the reality is that one clock, UTC(NIST), was used for both.

There are two sets of clocks involved in GPS: those belonging to the GPS satellites and those belonging to the

receivers on the ground. These clocks are not synchronized to each other, and since, in GPS, clocks are used to measure distance, this must be taken into account in the estimation process.

In a regional network containing multiple GPS receivers, the customary method for handling this is to treat one of the receiver clocks as being perfect and to estimate the time offsets of the other receiver and satellite clocks relative to it [5]. The clock held fixed is typically referred to as the "reference" clock. However, because we had only two receivers and a very short baseline, we chose a different approach: rather than estimating satellite-clock offsets, we chose to fix these values to a precise table of corrections already computed by JPL. This defined the reference clock in our analysis to be the reference clock used by JPL in estimating their satellite-clock corrections. We then estimated the offsets of our two receiver clocks relative to that reference clock.

The receiver-clock offsets were estimated once every five minutes as white-noise parameters. By "white noise" we mean that these parameters were modeled as if the value obtained at one epoch were completely independent of the value obtained at the next. Each 24 hours of data therefore yielded two 288-point time series: one corresponding to the time difference between the receiver clock at NIST_A and the reference clock, and another corresponding to the time difference between the receiver clock at NIST_B and the reference clock. Subtracting these yielded Clk(NIST_A) – Clk(NIST_B), the quantity of interest.

The time series Clk(NIST_A) – Clk(NIST_B) has a constant remaining in it because we have not accounted for cable and equipment delays. However, the slope of the time series should accurately represent the frequency difference between the two receiver clocks. Since we have used UTC(NIST) to run each of the receivers, the expected slope is zero.

IV. Results

Fig. 2 shows each of the daily time series obtained for Clk(NIST_A) – Clk(NIST_B) for the days 5-9 October 2002. Fig. 3 shows a similar set of results for the days 19-25 October 2002. We have fitted a least-squares line to each day's results and have labeled each day's results with the slope of that line. The uncertainties of the slope values are 4-6 ps/d. A single constant was removed from all of the data in Fig. 2, and a different constant was removed from all of the data in Fig. 3.

In both plots, there are small jumps in time between the end of one day and the beginning of the next that can be ignored. These so-called "day-boundary offsets" are caused by the impact of pseudorange noise on the fact that we arbitrarily cut satellite arcs in two at midnight, a subject that will be revisited briefly in section V_A.

As Figs. 2 and 3 show, our results have a non-zero slope. We begin by looking at the data in Fig. 3 since they are less problematic.

The time series obtained for 19 and 20 October have very large slopes: 211 ps/d and 105 ps/d, respectively. However, the multiplier on the NIST_A receiver malfunctioned between 17 and 18 October, and after replacing it, we restarted data collection on 18 October at about 18:00 UTC. That was only six hours prior to the start of Fig. 3, and therefore it's possible that the large slopes of 19 and 20 October reflect some sort of after-effect of the malfunction and replacement.

The results shown from about 22 October onward, while not excellent, are reasonable. We obtain smallish slope values—12-24 ps/d—which (a) meet our bare-minimum accuracy requirement of 43 ps/d and (b) do so in an averaging time of one day. Furthermore, some of the slopes are positive and some are negative. This is important

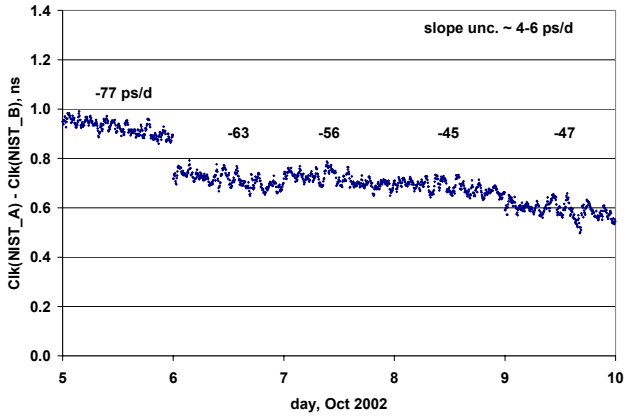

Fig. 2. Common-clock results obtained for 5-9 October 2002. The y axis shows the GPS-derived time difference between the clock running the NIST_A receiver and the clock running the NIST_B receiver. These are actually the same clock, UTC(NIST). A single constant has been removed from all of the data in this plot; the jumps between daily solutions can be ignored. Each of the daily solutions is labeled with a number that denotes the slope of a least-squares line fit to that solution; the uncertainties of the slopes are about 4-6 ps/d.

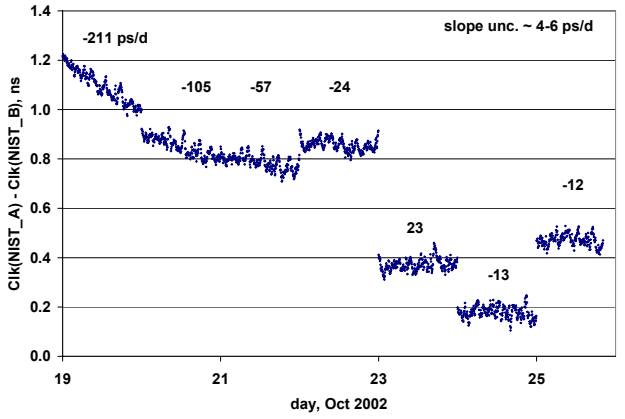

Fig. 3. Common-clock results obtained for 19-25 October 2002. The same as Fig. 2, but for data recorded two weeks later. The x axis in this plot is more compressed than the x axis in Fig. 2; the y axes of the two plots are the same.

because if we do have errors in the GPS-derived frequency, we would like them to ultimately average out to zero.

We now set these data aside and look at Fig. 2. While none of the slopes in Fig. 2 are enormous, these data possess the unfortunate characteristic that all of the slopes are fairly large (47-77 ps/d) and all of them are negative. Thus, it appears that a systematic frequency error has arisen in either the measurement or data-analysis process, and as such, there's no indication that this error would ultimately average out to zero.

Our attempts to discover the source of this error are the focus of the remainder of this paper.

V. Discussion

When considering the data obtained for 5-9 October 2002, several possibilities suggest themselves. Thus far, we have investigated three. In order of increasing complexity, they are:

A. *Uneven sampling rates*: during this period, the NIST_A receiver recorded data every two seconds and the NIST_B receiver recorded data every 30 seconds, whereas during 19-25 October 2002, both receivers recorded data every 30 seconds.

B. *Satellite-clock corrections*: perhaps it would have been better to estimate these parameters rather than fixing them to predetermined values.

C. *Wet zenith tropospheric delays*: perhaps these parameters have been estimated incorrectly.

We evaluate each of these in turn.

A. Sampling rates

It is difficult to imagine why this should be an issue. However, sampling rate does affect the software's ability to detect and repair cycle slips: generally, the higher the sampling rate, the better *GIPSY* is able to distinguish cycle slips from ionospheric noise. Furthermore, sampling rate also plays a role in the carrier-smoothing of the pseudorange measurements: the pseudorange measurements are carrier-smoothed from their original sampling rate of one point every two (or 30) seconds down to their final rate of one point every 5 minutes. Therefore, when the original sampling rate is higher, more pseudorange points are averaged together to form a single 5-minute data point. This should result in a better averaging-down of the pseudorange noise.

Because the NIST_A receiver had a higher sampling rate, the data from this receiver should have received better cycle-slip repair and pseudorange-noise averaging than the data from the NIST_B receiver. Again, it is difficult to understand how this might cause a systematic rate error, but we investigated it nonetheless.

To see whether we could remove the systematic error by forcing the initial rates to be the same, we re-converted the raw binary Ashtech data from the NIST_A receiver to RINEX, but this time, we saved only the measurements that occurred on the zero- and 30-second points of each minute. We then re-analyzed the NIST_A and NIST_B data with the two data files having identical 30-second data epochs from the start.

Figs. 4a and 4b show the results. Fig. 4a is a replica of Fig. 2, but with the data plotted on a smaller y-axis scale: it shows the answers obtained when the data files had different sampling rates. Fig. 4b shows the answers obtained when the NIST_A data were pre-decimated to a 30-second sampling rate so as to match the NIST_B data.

As these two figures show, pre-decimating the NIST_A data increased the size of some of the day-boundary offsets. That's not surprising: these jumps are thought to be caused by pseudorange noise [10], and by using fewer raw data points, *GIPSY* was less able to average down the pseudorange noise at the NIST_A receiver. Hence, larger offsets. However, pre-decimating the NIST_A data did not remove the slopes in the daily solutions and in fact had very

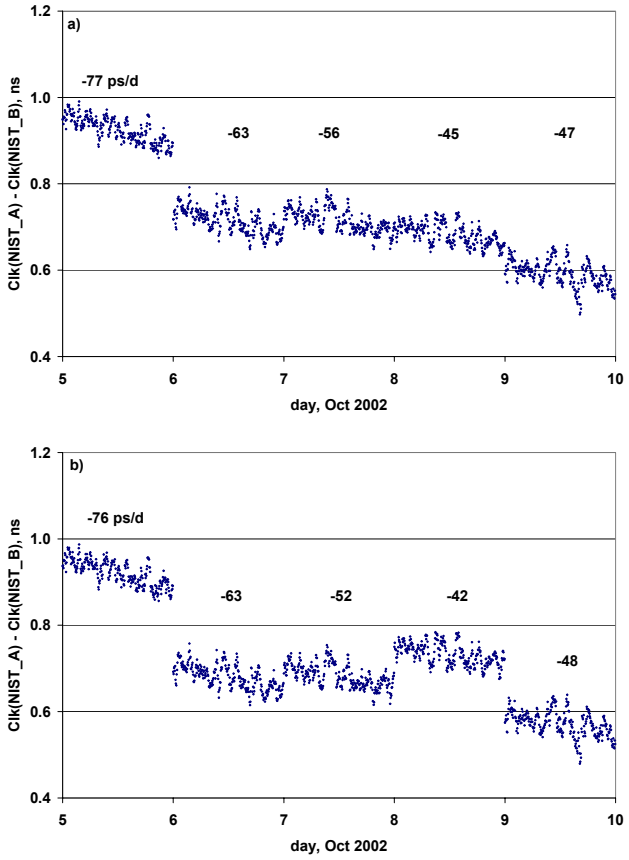

Fig. 4. Effect of unequal sampling rates on the clock solution. Fig. 4a shows the original solution in which the raw NIST_A data had been spaced at two-second intervals and the raw NIST_B data had been spaced at 30-second intervals. Fig. 4b shows the results obtained when the raw data from the NIST_A receiver were pre-decimated to a 30-second spacing so that the data from the two receivers had the same sampling rate throughout the entire analysis process.

little effect on the values of the slopes. Thus, it does not appear that the uneven sampling rates caused the systematic frequency errors.

B. Estimating satellite-clock corrections

As mentioned earlier, we chose to fix the satellite-clock corrections to predetermined values as opposed to choosing the more-established procedure of estimating them. We now discuss this choice in more detail and examine whether it was the source of our systematic frequency error.

We chose to fix satellite-clock corrections rather than estimating them because this made our analysis both simple and controlled. Had we chosen to estimate satellite-clock corrections, we would have had to add data from other GPS sites in order to obtain a statistically robust solution. This could have clouded our results. Furthermore, we felt this choice was justified in that our baseline was so short that the two receivers saw approximately the same GPS satellites at the same times. Thus, if there had been an error in the value of a satellite-clock correction, this error would have caused approximately the same error in the estimate of Clk(NIST_A) – reference clock as in the estimate of Clk(NIST_B) – reference clock. Hence, it would have canceled out when the two values were subtracted to form Clk(NIST_A) – Clk(NIST_B).

The facts remained, however, that (a) the two receivers did not see precisely the same satellites at the same times and (b) we had an unexplained systematic frequency error. Therefore, we tried fixing one receiver clock and estimating the satellite clocks and other receiver clocks relative to it to see whether this would remove the systematic error.

In order to do this, we added data from the three closest Ashtech stations available: TMGO (Table Mountain Gravity Observatory) in Boulder, Colorado; AMC2 in Colorado Springs, Colorado; and CASP in Casper, Wyoming. After adding the data from these three stations to our analysis, we re-estimated the parameters for each day, this time fixing the receiver clock at NIST_B and estimating the offset of the NIST_A receiver clock relative to it. The satellite clocks and the clocks of all the other ground stations were estimated relative to NIST_B as well.

Fig. 5 shows the results. In 5a, we again repeat Fig. 2, i.e., we show the results of the original analysis in which we had fixed the satellite-clock corrections. In 5b, we show the results obtained when the satellite-clock corrections were estimated. As expected, estimating satellite-clock corrections (rather than fixing them) made very little difference in the answer. Thus, we do not believe that using pre-determined values for the satellite-clock corrections caused our systematic frequency error.

C. Wet zenith tropospheric delay

Unlike the issues of sampling rates and satellite clocks, estimating the tropospheric delay incorrectly has real potential to corrupt a clock solution. That's because the error in the clock solution is proportional to the error in the estimate of the tropospheric delay.

The two are related by the following equation:

$$dCLK = -3.4 \cdot dZTD \quad (1)$$

where dZTD represents the error in the zenith tropospheric delay and dCLK represents the resulting error in the clock estimate [11].

To illustrate: in our analysis, we estimated two independent time series for the wet zenith tropospheric delay: one for NIST_A and one for NIST_B. Suppose that at a given epoch, we had somehow made an error in either (or both) of these values so that when we subtracted the two values, the value obtained for the difference was in error by 6 mm from the true value of the difference.

Scaling by the speed of light, 6 mm = 20 ps. By applying Equation (1), we see that 6 mm (20 ps) of error in the relative tropospheric delay produces an error of -68 ps in the estimated value of Clk(NIST_A) – Clk(NIST_B).

If we were to estimate the relative tropospheric delay incorrectly but to do so in a consistent manner throughout the day, then this wouldn't cause an error in frequency: rather, it would manifest itself as merely another constant.

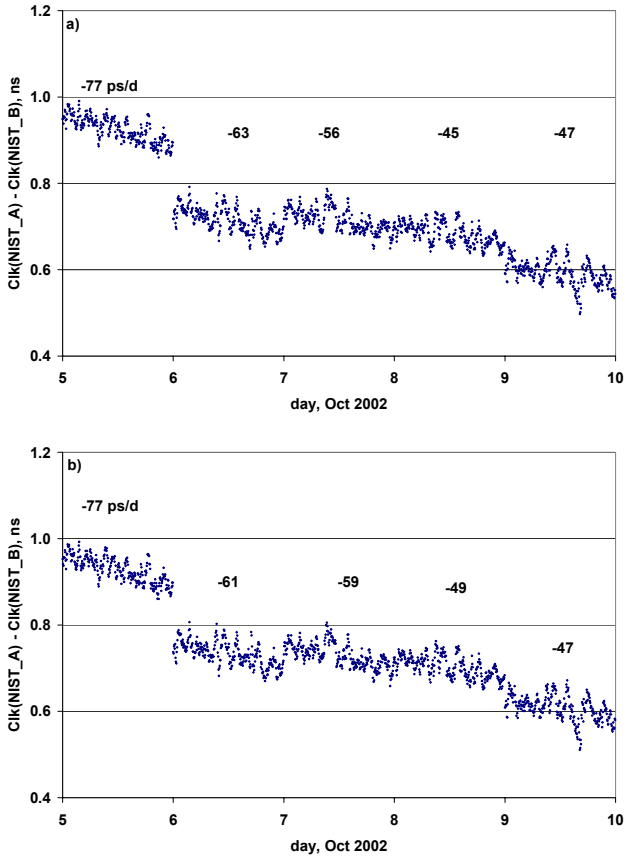

Fig. 5. Effect of estimating satellite-clock corrections. Fig. 5a shows the original solution in which we had fixed the satellite-clock corrections to the values obtained from JPL. Fig. 5b shows the results obtained when these corrections were estimated rather than fixed.

However, if the size of the error were to vary throughout the day, then this would introduce a frequency error into the relative clock solution.

Given the importance of estimating the tropospheric delay correctly, we tested two additional estimation procedures to see if either would improve the quality of our clock solutions.

1. Estimating a single common time series for the wet zenith tropospheric delay.

In the original analysis, we had estimated one time series for the wet zenith tropospheric delay at NIST_A and a separate time series for the wet zenith tropospheric delay at NIST_B. However, the NIST_A and NIST_B antennae were so close together that they should have experienced almost identical tropospheric delays. Therefore, we tested an estimation strategy in which we used the data from both receivers to estimate a single common time series for the wet zenith tropospheric delay. In other words, we allowed this parameter to vary with time, but we forced it to be the same at both receivers.

2. Fixing the tropospheric delay at both sites to be equal to an independently derived set of values.

This time, we didn't estimate the tropospheric delay. Rather, we fixed the total zenith tropospheric delay (wet + hydrostatic) at both sites to be equal to a set of total zenith tropospheric delay values computed by an external agency, the University Corporation for Atmospheric Research (UCAR). The UCAR values had a spacing of 30 minutes: they occurred on the hour and half-hour.

This seemed like a reasonable experiment because the imported tropospheric delays had been computed for a GPS site approximately 400 m away from our antennae. Furthermore, the height of that site differed from the taller of our two sites by only 6 m. Finally, the method used to obtain these tropospheric delays had been tested against water-vapor radiometry with the result that these values were thought to be accurate at the 1 cm level [12-14].

Figs. 6a-c show the results of our experiments. Fig. 6a once again repeats Fig. 2, thus showing the original case in which we had estimated separate time series for the wet zenith tropospheric delays at the NIST_A and NIST_B antennae. Fig. 6b shows the results obtained when the wet zenith tropospheric delay was estimated as a single time series common to both sites. Figure 6c shows the results obtained when the total zenith delay at each of the two sites was set equal to the value of the total zenith delay obtained from UCAR.

The data in Figs. 6b and 6c do show a reduced level of scatter. We believe this occurs because we are estimating fewer parameters. And, we do see a bit of improvement in the slopes on 5 and 9 October. However, neither of these strategies removes our systematic frequency error in a consistent manner.

We have experimented with a variety of other tropospheric estimation techniques, e.g. allowing for azimuthal asymmetry, varying the level of random-walk

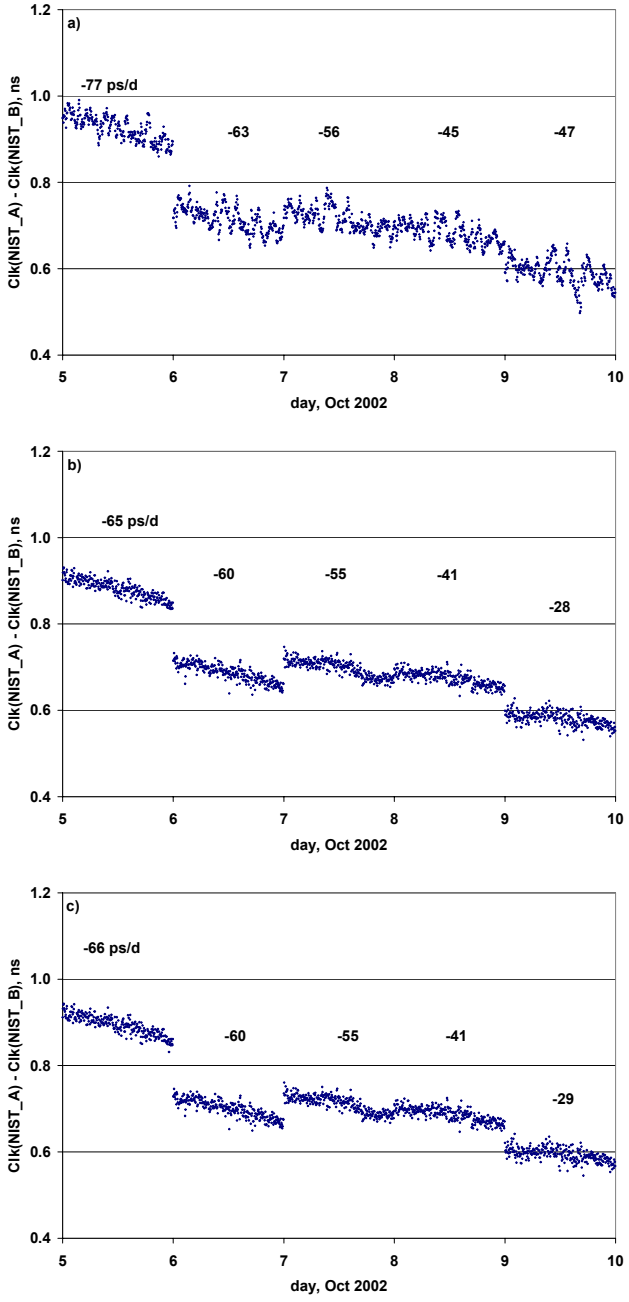

Fig. 6. Effect of changing the estimation of the wet zenith tropospheric delay. Fig. 6a shows the original solution in which we had estimated separate time series for the wet zenith tropospheric delays at the NIST_A and NIST_B antennae. Fig. 6b shows the results obtained when the wet zenith tropospheric delay was estimated a single time series common to both sites. Figure 6c shows the results obtained when the total zenith tropospheric delay at each of the two sites was set equal to the value of the total zenith tropospheric delay obtained from UCAR.

noise, estimating the tropospheric delay as a white-noise parameter, estimating the delay as a constant parameter or not at all, etc. None of these experiments have proved any more effective than those shown above.

It is still possible that we are estimating the tropospheric delay values incorrectly and that this is the sole cause of our systematic frequency error. However, since we haven't been able to find a tropospheric-estimation strategy that removes this systematic error, we aren't able to prove that this is the case. Furthermore, given that the problem has persisted in the face of a multitude of tropospheric-estimation strategies, we are beginning to suspect that the source of the error lies elsewhere.

VI. Conclusions and Future Work

A substantial portion of the results obtained in this experiment display systematic errors in frequency. We have not yet been able to identify the source of these errors. Therefore, we aren't yet able to consistently demonstrate the frequency accuracy required for the comparison of primary frequency standards.

It is possible that there is still some parameter-estimation strategy that will enable us to remove these systematic errors. For example, we have by no means exhausted the techniques available for estimating the tropospheric delay. However, we feel that it would be more beneficial to begin investigating antenna-, receiver- and site-specific effects such as multipath and temperature sensitivity.

As Fig. 2 shows, at first glance, each of the daily solutions appears to be a straight line with a non-zero slope. However, closer inspection reveals that there is often a part of the day which has a reasonably flat slope, but that this is then followed by a period in which the relative clock solution angles off. Fig. 7 shows an example of this in which the transition takes place at about 12:00 UTC.

If we can determine what causes that transition, we will almost certainly understand what lies at the root of the problem.

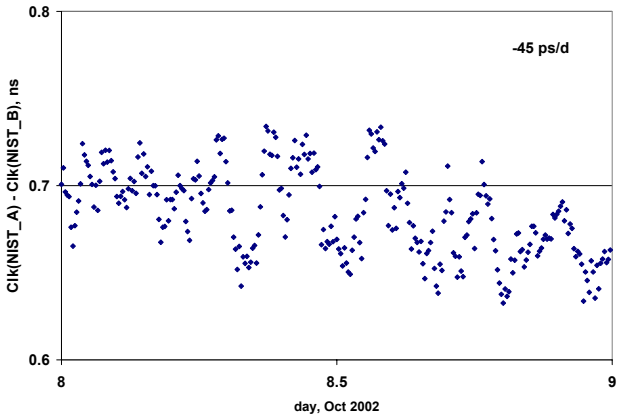

Fig. 7. Future work. The slope of the plot is relatively flat up until 12:00 UTC, at which time the clock solution begins to angle downward. We hope to determine what causes this transition.

Acknowledgment

The authors thank the BIPM for the use of its receiver. We also thank UCAR for providing values of the tropospheric delay.

References

[1] F. Overney, T. Schildknecht, G. Beutler, L. Prost, and U. Feller, "GPS time transfer using geodetic receivers: middle-term stability and temperature dependence of the signal delays," in *Proc. 11th Eur. Freq. Time Forum*, pp. 504-508, 1997.

[2] W. Gurtner, "RINEX: the receiver-independent exchange format," *GPS World*, vol. 5, pp. 48-52, 1994.

[3] L. Estey and C. Meertens, "TEQC: the multi-purpose toolkit for GPS/GLONASS data," *GPS Solutions*, vol. 3, pp. 42-49, 1999.

[4] F.H. Webb and J.F. Zumberge, editors, *An Introduction to GIPSY/OASIS-II: Precision Software for the Analysis of Data from the Global Positioning System*, JPL D-11088 (internal publication), Jet Propulsion Laboratory, Pasadena, CA, July 1997.

[5] K.M. Larson and J. Levine, "Carrier-phase time transfer," *IEEE Trans. UFFC*, vol. 48, pp. 1001-1012, 1999.

[6] P. Misra and P. Enge, *Global Positioning System: Signals, Measurements and Performance*, Lincoln, MA: Ganga-Jamuna Press, 2001.

[7] G. Blewitt, "Carrier-phase ambiguity resolution for the Global Positioning System applied to geodetic baselines up to 2000 km," *J. Geophys. Res*., vol. B94, pp. 10,187-10,203, 1989.

[8] Y.E. Bar-Sever, P.M. Kroger, and J.A. Borjesson, "Estimating horizontal gradients of tropospheric path delay with a single GPS receiver," *J. Geophys. Res.*, vol. B103, pp. 5019-5035, 1998.

[9] A.E. Niell, "Global mapping functions for the atmospheric delay at radio wavelengths," *J. Geophys. Res*., vol. B101, pp. 3227-3246, 1996.

[10] R. Dach, T. Schildknecht, T. Springer, G. Dudle, and L. Prost, "Continuous time transfer using GPS carrier phase," *IEEE Trans. UFFC*, vol. 49, pp. 1480-1490, 2002.

[11] *Y. Bar-Sever*, personal communication, 2003.

[12] C. Rocken, T. Van Hove, and R. Ware, "Near real-time GPS sensing of atmospheric water vapor," *Geophys. Res. Lett*., pp. 3221-3224, 1997.

[13] R. Ware, C. Alber, C. Rocken, and F. Solheim, "Sensing integrated water vapor along GPS ray paths," *Geophys. Res. Lett*., vol. 24, pp. 417-420, 1997.

[14] *T. Van Hove*, personal communication, 2003.